

How to Cite:

Kumar, S., Shankar, B., Saxena, S., RashmiTomar, Singh, M., Sahu, D. K., & Srivastava, A. K. (2022). Intrinsically conducting polymer nanocomposite as the vigorous material for the health monitoring. *International Journal of Health Sciences*, 6(S3), 10236–10247. <https://doi.org/10.53730/ijhs.v6nS3.8446>

Intrinsically conducting polymer nanocomposite as the vigorous material for the health monitoring

Shailesh Kumar

Department of Physics, Institute of Basic Science, Bundelkhand University Jhansi, India-284128

Bhawani Shankar

Department of Physics, Hansraj College University of Delhi, Delhi India-110007

Swasti Saxena

Department of physics, Sardar Vallabhbhai National Institute of Technology, Surat India 395007

RashmiTomar

Department of Chemistry, M. S. J. College, University of Rajasthan, Jaipur, India-321001

Manveer Singh

Department of Physics, Ramjas College University of Delhi, Delhi India-110007

D. K. Sahu*

Department of Physics, Raghuveer Singh PG College, Lalitpur, India-284403

Ankit Kumar Srivastava*

Department of Physics, Indrashil University, Mehsana 382740, India

Abstract--- Individual poly(methyl methacrylate)/MWCNT doped with sulfuric acid were polymerized in situ to yield individual nanotubes with increased electrical conductivity. In the presence of aliphatic alcohol vapors of various diameters, the Nanocomposites were measured as a function of time. These sensor responses are particularly rapid due to the huge surface to volume ratio, consistent diameter, and limited amount of active material employed in the design. Individual nanotube sensors demonstrate actual saturation when exposed to and removed from the detecting gas. In addition, a chemical sensing system was created employing a nanocomposite film in both air and vapor alcohol gas. When exposed to alcohol, the surface reaction was immediate, with virtually total current recovery

after pumping out the alcohol, making it a reusable sensor with rectifying behaviour.

Keywords---poly methyl methacrylate, PMMA, nanocomposites, chemiresistive sensors, multiwalled carbon nanotubes.

Introduction

A slew of recent research have focused on the use of nanomaterials to many medical fields, spawning a new field known as nanomedicine. It includes employing nanomaterials to diagnose, treat, cure, and prevent illnesses, as well as dealing with traumatic damage, pain relief, and preserving/improving human health. Natural and manmade polymer nanocomposites have a significant position among nano materials. An organic polymer matrix and mineral, organic, or metallic nanofiller make up these. The properties of polymer nanocomposites are determined by the components' characteristics as well as the polymer-nanofiller interaction. Polymer nanocomposites provide new prospects for antibacterial treatment, tissue engineering, cancer therapy, medical imaging, dental uses, drug administration, and other applications in contemporary medicine.

To successfully avoid any widespread loss of life and property, rapid detection of minute quantities of dangerous gases in an insufficiently ventilated environment is crucial. This necessitates sensors that can detect minute amounts of gas, such as those made from nanocomposites with a high surface-to-volume ratio. For a number of reasons, intrinsically organic conducting polymers (ICPs) are particularly well suited for use as gas sensors. The oxidation/reduction states of these polymers, in particular, may be reversibly modified by exposing them to basic/acidic environments, resulting in a shift in conductivity of many orders of magnitude [1] with no polymer degradation, extending the lifespan of sensors based on these polymers. Furthermore, ICPs are inexpensive and simple to make in large quantities, are reasonably stable in ambient settings, and may be easily processed into films. Individual poly(methyl methacrylate) (PMMA) and Multiwalled carbon nanotube (MWCNT) and PMMA/MWCNT nanocomposites were utilised to sense a range of alcohols with response times that were quicker than sensors produced from thin films of the same material [2,3]. The compact size and possibility for better sensitivity of a nanocomposite film chemical sensor are advantages.

The PMMA/MWCNT sensors were more resilient than the other conducting polymer nano nanocomposite sensors and could be utilised numerous times for sensing various aliphatic groups. After using the PMMA-MWCNT sensors in any gas, the response was lowered, therefore it was recommended to utilise a new sensor for various gas detecting. The possibility to fabricate lengthy nanocomposites of conducting polymers by chemical method with a high aspect ratio and even bigger surface to volume ratio makes this technology particularly appealing for application in the construction of film, low power consumption, and fast response gas sensors. As a result, multifunctional film may be produced, increasing their versatility. Intrinsically conducting polymers (ICPs) with a large

range of conductivity (10⁻⁵-10³ S/cm) have fascinating optical and mechanical features in addition to metallic conductivity. As a result, these conducting polymers might be employed to replace inorganic sensing materials. The flexibility, tailorability, adaptability, low weight, and chemical stability of conducting polymers over inorganic materials are all significant benefits.

Materials and Method

The MWCNTs were utilised as obtained from Aldrich (purity 95%, diameter 10-15 nm, length 0.1-10 μ m, density 1.7-2.1 g/cm³, batch 05225JA). Prior to usage, Meta aminophenol (Merck, India) was distilled at low pressure. Without additional purification, reagent grade ammonium persulfate, hydrochloric acid, sulphuric acid and nitric acid (Merck, India) were employed. The synthesis and washing were done with deionized water.

PMMA-MWCNT nanocomposites synthesis and film casting

The MWCNTs dispersed aqueous 0.6 (M) NaOH medium was used to create PMMA-MWCNT nanocomposites with varied weight percentages of MWCNTs (viz. 1, 2, 3, 4, and 5wt percent) using ammonium persulfate oxidant, as previously described [5]. MWCNTs were first disseminated well in 50 mL of aqueous 0.6 (M) NaOH solution using a continuous probe ultrasonication for 10-15 minutes. By aggressively magnetic stirring, the m-aminophenol monomer (3.27 g, 10 mmol) was dissolved in MWCNTs dispersed aqueous NaOH medium in a two-necked round bottom flask (RB). Freshly made ammonium persulfate (10.27 g, 15 mmol) solution in water (25 ml) was added to the aforementioned mixture one at a time and left to react for 8-10 hours at room temperature with continual stirring. The deep brown precipitate of PMMA-MWCNTs nanocomposites was filtered and washed vigorously with 4 (M) HCl followed by deionized water until the pH of the filtrate became neutral in order to eliminate unreacted monomers, by-products, or oligomers.

The blackish brown product was then dried for 7-8 hours in a vacuum thermal chamber at 70-80°C. T11, T31, and T51 are the designations for PMMA-MWCNT nanocomposites containing 1, 3, and 5 wt percent MWCNTs, respectively. Sulfuric acid [1:1] doping improves the conductivity properties of T11, T31, and T51. By stirring, the 0.7-0.8 g PMMA-MWCNT powder was dissolved in 10-15 ml DMSO and put onto a well-clean flat glass petridish with a diameter of 10 cm. The petridish was then put in a vacuum thermal chamber for 7-8 hours at 80-90°C. A blackish coating produced once the solvent was completely evaporated. The film was dipped 5/6 times alternatively in deionized water and acetone to remove retained DMSO. The film was properly dried in a vacuum oven and characterised in a vacuum desiccator.

Characterization of PMMA -MWCNT nanocomposites

Table 1 shows the compositions, crude yields, intrinsic viscosities, and DC-conductivities of PMMA-MWCNT nanocomposites produced using the procedure described in the preceding section. The temperature rises with time during the synthesis of nanocomposites, similar to the polymerization of MMA, and reaches a

maximum of 80-90°C in 3-4 minutes in the case of all nanocomposites. The MWCNT does not appear to interfere with the extremely quick polymerization process. The intrinsic viscosity $[\eta]$ of the PMMA and PMMA-MWCNT nanocomposites was calculated using a plot of specific viscosity/concentration (η_{sp}/C) vs polymer concentration at infinite dilution to compare polymer chain growth.

All of the samples had straight line graphs that followed Huggins' equation. The inherent viscosity and % yield of PMMA and PMMA-MWCNT nanocomposites are similar (Table 1). As a result, the polymer chain development is nearly identical in all nanocomposites. The nanocomposite containing 5 wt % MWCNT had the greatest inherent viscosity as well as percent yields (Table 1). This was most likely owing to better directed polymerization for better MWCNT-PMMA interaction, which resulted in less oligomer than previous nanocomposites. In DMSO and DMF, all of the samples are very soluble. Nanocomposites, like PMMA, are soluble in concentrated aqueous basic solution. It is feasible to cast films from DMF or DMSO solutions. The above observations confirm the nanocomposites have similar solubility and film forming properties like PMMA and therefore MWCNT don't have any adverse effect on the properties of the polymer.

Table 1
Compositions, crude yields, intrinsic viscosities, and DC-conductivities for the synthesized samples

Sample	% wt MWCNT	% yields	$[\eta]$ (dL/g)	$\sigma \times 10^8$ (S/cm)
PMMA	0	86.4	0.127	$<10^{-4}$
PC1	1	87.0	0.05	2.71
PC2	2	84.0	0.16	13.32
PC3	3	83.0	0.09	2.93
PC4	4	87.2	0.08	3.33
PC5	5	85.6	0.08	4.30

Figure 1 shows the UV-VIS spectra of PMMA and PMMA-MWCNT nanocomposites doped with sulfuric acid [1:1] to determine the interaction between the MWCNT and the PMMA matrix. The absorption unit of pure PMMA is showed only one characteristic peaks at ~ 340 nm for $\pi - \pi^*$ transitions [6]. However, this characteristic absorption maximum for $\pi - \pi^*$ transitions are observed very weak or vanished in the spectra of PMMA-MWCNT nanocomposites. The additional absorption peak of $n-\pi^*$ becomes prominent in the PMMA -MWCNT nanocomposites at around 280nm is expected to arise from the charge unit between nonbonding electron of PMMA associated with $-OH$ or $-N-$ moieties and MWCNTs [7,8]. Furthermore, the peak's saturation is maximum for T51, i.e., the nanocomposite with 5% MWCNT concentration, indicating the best or most efficient charge transfer between PMMA and MWCNTs.

As a result, UV-VIS spectrum measurements show that charge transfer interactions between the PMMA layer and MWCNTs in the produced PMMA-MWCNT nanocomposites cause induced doping. The UV-VIS spectra of the monomer and MWCNT combination in the reaction media may be used to validate the formation of such a charge transfer complex before polymerization. The donor

-O- or lone pair on -N- of MMA is firmly coupled with the acceptor MWCNT in aqueous NaOH medium via significant charge transfer. The red shift of transition maxima in UV-VIS spectra for PMMA in NaOH medium at 340 nm to 350 nm for doping in sulfuric acid PMMA /MWCNT in NaOH media confirms this.

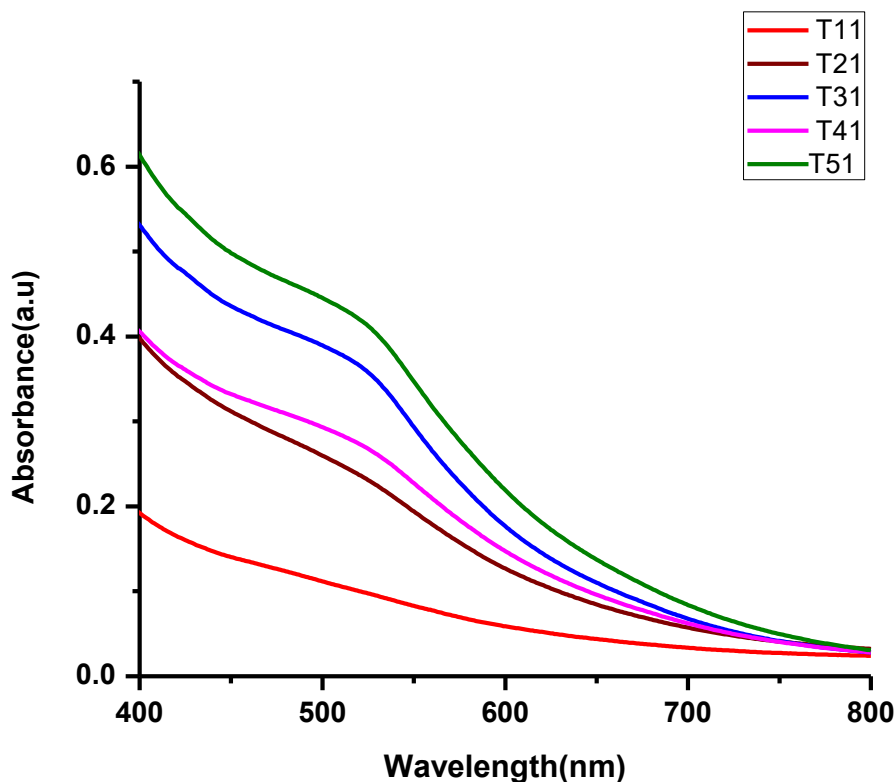


Fig 1. UV -VIS diagram of doping sulphuric acid nanocomposite $C \equiv N$ cm^{-1}

Figure 2 shows the FTIR spectra of PMMA and PMMA-MWCNT nanocomposites. Figure 2 shows that the produced PMMA/MWCNT doping in sulfuric acid nanocomposites has similar peak locations associated with the PMMA structure in the 2200-400 cm^{-1} range. The significant bands between 1600 and 1520 cm^{-1} in this area are typical stretching bands of the $C \equiv N$ quinoid and benzenoid structures, respectively. The charge delocalization across the polymeric backbone causes the strong absorption band about 1220 cm^{-1} (C-N stretching) [5]. When compared to PMMA, the widening powerful peak at that location in the nanocomposite shows the substantial charge delocalization over the polymeric backbone caused by MWCNT inclusion. PMMA and PMMA -MWCNTs have quite distinct peak positions in the 4000-2000 cm^{-1} range.

For all nanocomposite samples, the wide stretching band of aromatic C-H, hydrogen bonded -OH, and -NH- groups for PMMA at 3490, 3322, 3121 cm^{-1} is displaced to 3300, 2900, 2400 cm^{-1} , respectively. The significant charge transfer interactions between the -conjugated surfaces of MWCNT and the -OH and -N-

moieties of PMMA in their composites can be attributed to this [6,7]. The enlargement of the characteristic peak owing to interaction of MWCNT with the phenoxide ion of monomer in basic media [1] predicts substantial charge transfer through free $-OH$ groups.

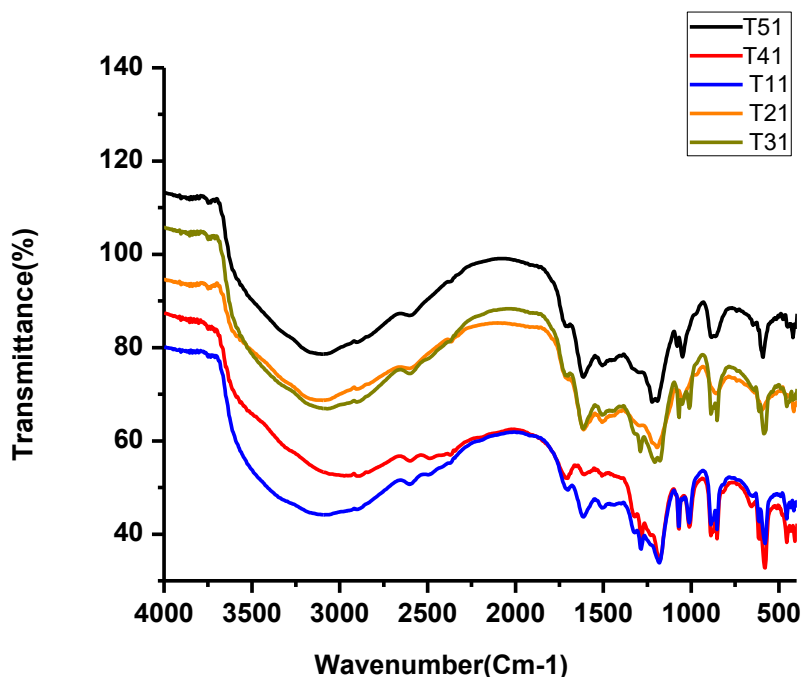


Fig 2. FTIR diagram of doping sulphuric acid nanocomposite wt% of MWCNT

Figure 3 depicts SEM micrographs of PMMA-MWCNT nanocomposites, whereas Figure 4 depicts a dark field TEM picture of T11, T31, and T51 nanocomposites. The high specific surface area of nanotubes affords a large number of sorption sites for PMMA monomer, which can polymerize to create a coating over the nanotubes. PMMA chains coiled the MWCNT tubes exist as beads at low MWCNT concentrations (Figure 3). This is due to the strong attachment of PMMA to the MWCNT surface in basic polymerization media, as well as the catalytic impact of the MWCNT surface. This is because the electron acceptor MWCNT and the electron donor $-O-$ and lone pair on $-N-$ of PMMA monomer in basic polymerization media produce a weak charge transfer complex [8]. This produces a PMMA-coated MWCNT bead, which causes exclusive surface polymerization [9]. Because of the high surface free energy, the aggregation propensity of nanotubes increases with increasing nanotube concentration, the size of the bead steadily increases with increasing MWCNT weight %. The average diameters of the nanotubes are improved by 5nm when the MWCNT weight percentage is increased from 1 to 5%, as demonstrated in the TEM micrograph (Figure 4). The size difference in T51 with 5% MWCNT is likely owing to less PMMA coating on MWCNT because to the high concentration of MWCNT. As a result, it is envisaged that e induced doping by charge transfer interactions between the PMMA layer and the MWCNTs will be strongest for T51 [10-12].

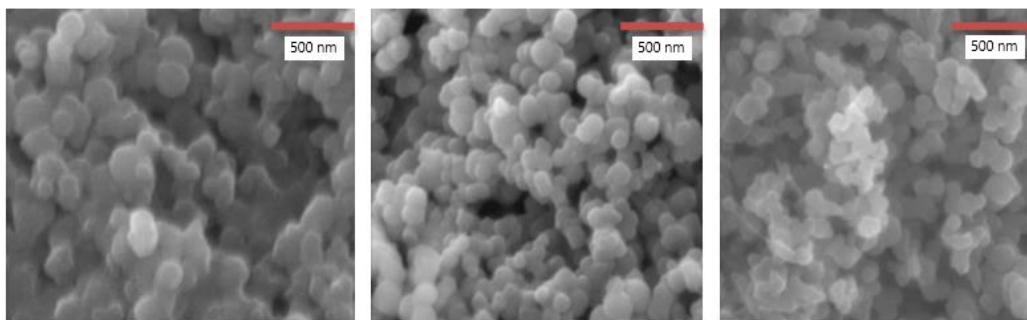


Figure 3. SEM images of PMMA-MWCNT nanocomposites (a) T11 (b) T31 (c) T51

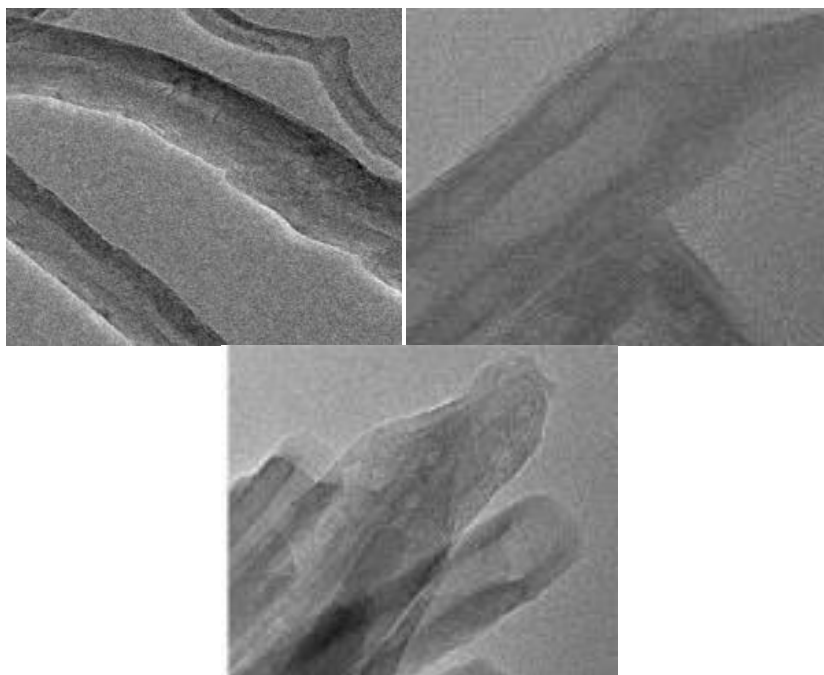


Figure 4. TEM micrographs of PMMA -MWCNT nanocomposites at 20nm scale (a) T11 (b) T31 (c) T51

Characterization of MWCNTs/PMMA nanocomposites doped in sulfuric acid

The process for making PMMA-MWCNT nanocomposites was discussed in the preceding section. Table 1 shows the weight % of MWCNT, crude yields, and intrinsic viscosities. The temperature rises with time during the synthesis of nanocomposites, similar to the polymerization of MMA, and reaches a maximum of 90-95°C in 5-8 minutes in the case of all nanocomposites. The MWCNT does not appear to interfere with the extremely quick polymerization process. The intrinsic viscosity $[\eta]$ of the PMMA and PMMA -MWCNT nanocomposites was calculated using a plot of specific viscosity/concentration (η_{sp}/C) vs polymer concentration at infinite dilution to compare polymer chain growth. All of the samples had straight line graphs that followed Huggins' equation. The inherent

viscosity and percent yield of PMMA and PMMA -fMWCNT nanocomposites are similar (Table 2).

As a result, the polymer chain development is nearly identical in all nanocomposites. This was likely due to better directed polymerization, which resulted in less oligomer than previous nanocomposites, allowing for greater interaction between sulfuric acid MWCNT doping and PMMA. In DMSO and DMF, all of the samples are very soluble. Nanocomposites, like PMMA, are soluble in concentrated aqueous basic solution. It is feasible to cast films from DMF or DMSO solutions. The foregoing findings show that nanocomposites have similar solubility and film-forming capabilities to PMMA, indicating that f -MWCNT has no negative impact on polymerization.

Table 2

For the synthesised samples, the weight % of MWCNT, crude yields, intrinsic viscosities, and DC-conductivities were calculated

Sample	% wt MWCNT	% yields	$[\eta]$ (dL/g)
PMMA	0	84.4	0.1927
T11	1	75.0	0.10
T31	3	84.0	0.13
T51	5	74.6	0.09

FTIR analysis was used to investigate the structural changes in carbon nanotubes following surface treatment. In compared to the spectrum of pristine, the spectra of fMWCNT revealed additional absorption bands at 1727, 1182, and 1025 cm^{-1} , as seen in Figure 2.

Properties: Mechanism for aliphatic alcohol vapor sensing

The detecting capabilities of the alcohol vapor sensing features of PMMA/Mwcnt for 500 ppm quantities of ethanol vapor in air was investigated in this study. During alcohol sensing, the resistivity of the polymer nanocomposite film falls and becomes constant saturation, whereas the resistivity of the polymer increases during alcohol changing from an adsorbed state on a surface to a gaseous or liquid state by air. However, because of the alcohol vapor absorption process, the crystallinity of the polymer reduces. The -OH groups of Ethanol molecules arrive to hydrogen bonded with the phenolic -OH group present in the polymer molecule. The hydrogen bonding a weak electron contribution effect occurs through the -OH group to the polymer chain and finally the electron flow throughout the polymer chain increases. The hydrogen bonding of alcohol molecules with =NH⁺ - groups is difficult due to the presence of bulky SO₄²⁻ counter ions of sulfuric acid dopant.

The PMMA/MWCNTT nanocomposites sensor, on the other hand, has a steady baseline (PANI) and better responses to alcohol vapors at all concentrations beyond that. The MWCNT interacts well with conjugated PMMA chains, paving the way for strong dipole interactions with the analyte molecule. Because of the interaction between conjugated polymer and MWCNT, the inherent electrical characteristics of MWCNT improved by PMMA play a key role in increasing

alcohol sensing performance. The resistance of the nanocomposite sensor is reduced due to electron delocalization and charge transfer via the PMMA. In the absence of alcohol, the usual responses of the PMMA /MWCNT (1-5 wt%) sensor air exposures. After three cycles of repeated exposure and removal of alcohol vapor, the nanocomposite sensor demonstrated high repeatability and reversibility.

The PMMA/MWCNT sensor's methanol& ethanol sensitivity is clearly improved when MWCNT concentrations rise. Because there are more interactions sites inside the nanocomposites sensor for alcohol detection, greater MWCNT concentrations result in more alcohol absorptions. Because of the synergetic effects between each component, these nanocomposite may be employed efficiently for alcohol sensing. Excellent sensitivity and selectivity to alcohol gas were achieved thanks to the good combination and synergetic behaviour of both components, which also improved the sensing response to nanocomposites.

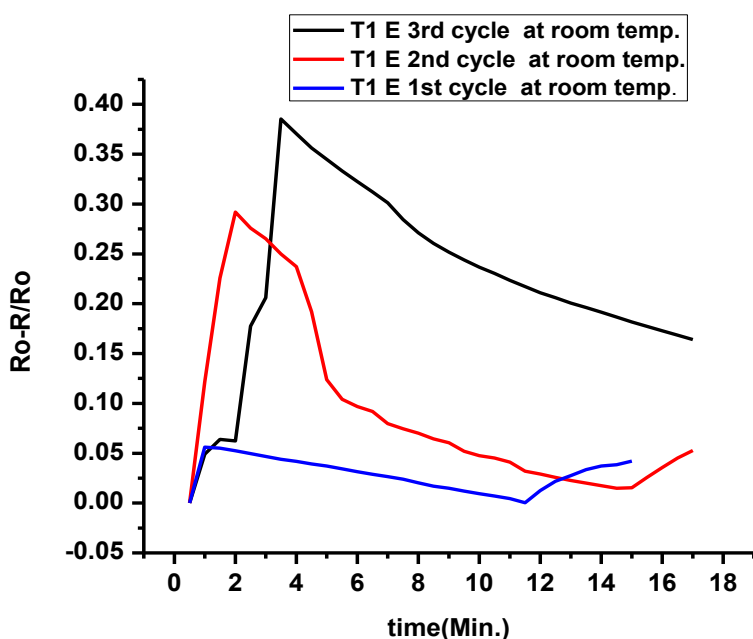


Fig 5 a. Sensing reproducibility of the 1wt% MWCNT-contained PMMA /MWCNT nanocomposite to 500 ppm at room temperature Ethanol

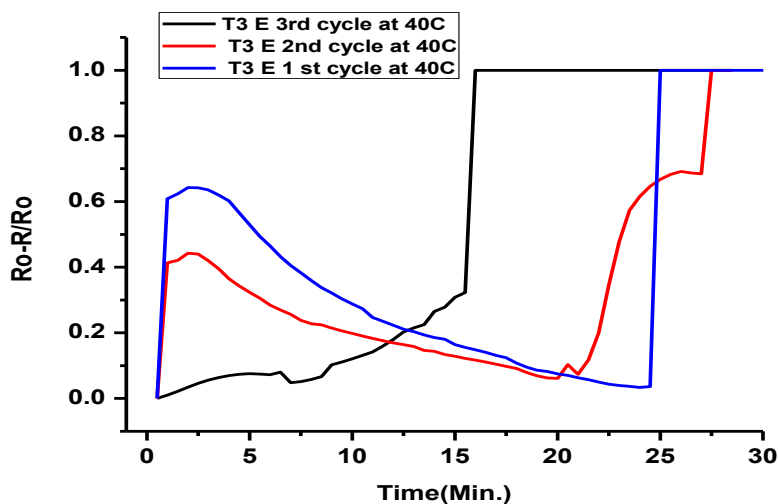


Fig5b. Sensing reproducibility of the 3wt% MWCNT-contained PMMA /MWCNT nanocomposite to 500 ppm at room temp Ethanol

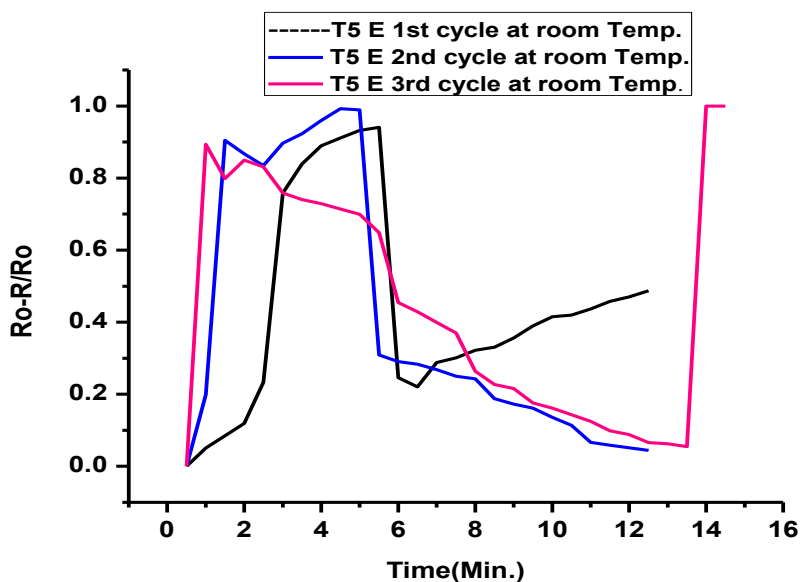


Fig 5c. Sensing reproducibility of the 5wt% MWCNT-contained PMMA /MWCNT nanocomposite to 500 ppm at room temp. Ethanol

Conclusion

A conducting polymer nanocomposite using MWCNT as a nanofiller was used to create a temperature sensor. The effects of MWCNT content (in the range of 1-5 wt%) on electrical resistance were thoroughly explored. At 3wt % MWCNT concentration, the resistance rises with the addition of alcohol. Physical,

chemical, and biological sensing applications may be possible using room-temperature produced p-doped PMMA–MWCNT nanocomposites [13-15].

In the presence of DMSO, PANi derivatives of PMMA–MWCNT nanocomposites were effectively produced. DMSO is used to boost the solubility of 2-aminophenol monomer, as well as to promote the dispersion of MWCNTs and as PMMA counterions. The homogeneous coating of PMMA–MWCNTs is confirmed by SEM images. This class of nanocomposites is thought to contribute to making point-of-care systems more inexpensive by leveraging the low cost and extrinsic (dopant- and redox-dependent) electrical characteristics of the PMMA–MWCNT. However, because the given sensing material is sensitive to environmental conditions like temperature, humidity, and stress, a designer must consider a variety of compensating strategies to reduce undesired sensor responses.

References

1. Chiang J C and Mac Diarmid A G, Polyaniline: Protonic acid doping of the emeraldine form to the metallic regime, *Synth Metals* 13, (1986) 193-205.
2. Pinto N J, Ramos I, Rojas R, Wang P-C and Johnson A T Jr., Electric response of isolated electrospun polyaniline nanofibersto vapors of aliphatic alcohols , *Sens Actuat B* 129 (2008) 621-627 .
3. Pinto N J, Rivera D, Melendez A, Ramos I, Lim J H and Johnson A T C, Electrical response of electrospun PEDOT- PSSA nanofibers to organic and inorganic gase Sensor Actuator B 156 (2011) 849-853.
4. Pinto N J, González R, Johnson A T Jr and Mac Diarmid A G, Dual Input AND gate fabricated from a single channel poly (3 hexylthiophene)thin film field effect transistor, *Appl Phys Lett* 89 (2006) 033505.
5. P. Kar, N.C. Pradhan, B. Adhikari, A novel route for the synthesis of processable conducting poly (m-aminophenol), *Mater. Chem. Phys.* 111 (2008) 59–64.
6. [6] L. Kong, X. Lu, W. Zhang, Facile synthesis of multifunctional multiwalled carbonnanotubes/Fe₃O₄ nanoparticles/polyaniline composite nanotubes. *J. Solid State Chem.* 181 (2008) 628–636.
7. Gopalan AI, Lee KP, Santhosh P, Kim KS, Nho YC. Different types of molecular interactions in carbon nanotube/conducting polymer composites—a close analysis. *Compos Sci Technol*; 67 (5) (2007) 900–5.
8. Jeevananda T, Siddaramaiah, Kim NH, Heo SB, Lee JH. Synthesis and characterization of polyaniline-multiwalled carbon nanotube nanocomposites in the presence of sodium dodecyl sulfate. *Polym Adv Technol*;19(12) (2008)1754–62.
9. P. Saini, R. Jalan, S.K. Dhawan, Synthesis and characterization of processable polyaniline doped with novel dopant NaSIPA , *J. Appl. Polym. Sci.* 108 (2008) 1437.
10. E.N. Konyushenko, J. Stejskal, M. Trchova, J. Hradil, J. Kovařir`ova`ı, J. Prokes`, M. Cieslar, J.-Y. Hwang, K.-H. Chen, I. Sapurina, Polyaniline nanotubes: conditions of formation, *Polymer* 47 (2006) 5715.
11. X.S. Du, M. Xiao, Y.Z. Meng, Facile synthesis of highly conductive polyaniline/graphite nanocomposites, *Eur. Polym. J.* 40 (2004) 1489.
12. J.E. Huang, X.H. Li, J.C. Xu, H.L. Li, Well-dispersed single-walled carbon nanotube/polyaniline composite films, *Carbon* 41 (2003) 2731.

13. P. Saini, V. Choudhary, B.P. Singh, R.B. Mathur, S.K. Dhawan, Polyaniline-MWCNT nanocomposites for microwave absorption and EMI shielding, *Mater. Chem. Phys.* 113 (2009) 919–926.
14. Wu TM, Lin YW. Doped polyaniline/multi-walled carbon nanotube composites: Preparation, characterization and properties. *Polymer*, 47(10), (2006) 3576-3582.
15. Mawhinney DB, Naumenko V, Kuzenetsova A, Yates Jr JT, Liu J, Smalley RE. Infrared spectral evidence for the etching of carbon nanotubes: Ozone oxidation at 298 K. *J Am Chem Soc*;122(10) (2000) 2383-2384.